

Angle-resolved photoemission study of the metal-insulator transition in bismuth cobaltates

Z. Yusof,^{1,*} B. O. Wells,¹ T. Valla,² P. D. Johnson,² A. V. Fedorov,^{2,†} Q. Li,³ S. M. Loureiro,⁴ and R. J. Cava⁴

¹*Department of Physics, University of Connecticut, 2152 Hillside Road U-46, Storrs, Connecticut 06269-3046, USA*

²*Physics Department, Brookhaven National Laboratory, Building 510B, Upton, New York 11973-5000, USA*

³*Division of Materials Sciences, Brookhaven National Laboratory, Upton, New York 11973-5000, USA*

⁴*Department of Chemistry and Materials Institute, Princeton University, Princeton, New Jersey 08544, USA*

(Received 11 October 2006; revised manuscript received 23 May 2007; published 15 October 2007)

We present an angle-resolved photoemission spectroscopy study of a Mott-Hubbard-type bismuth cobaltate system across a metal-insulator transition. By varying the amount of Pb substitution and by doping with Sr or Ba cation, a range of insulating to metallic properties is obtained. The electronic structure shows the emergence of a weakly dispersing state at the Fermi energy with increasing conductivity. A systematic change in the spectral weight of the coherent and incoherent parts, accompanied by an energy shift of the incoherent part, is also observed. The changes may be correlated with changes in the temperature-dependent resistivity. The nature of the coherent-incoherent components is compared to the peak-dip-hump feature seen in cuprate superconductors.

DOI: [10.1103/PhysRevB.76.165115](https://doi.org/10.1103/PhysRevB.76.165115)

PACS number(s): 71.30.+h, 79.60.-i, 71.28.+d

The metal-insulator transition (MIT) in strongly correlated electron systems is one of the central issues in condensed matter physics, particularly in areas such as the high- T_c superconductors and colossal magnetoresistance manganites. An important step to understand the nature of charge transport in such materials would be to understand and predict the single-particle excitation spectrum as measured by angle-resolved photoemission spectroscopy (ARPES). However, in many materials there are a variety of complications to the ARPES spectra making direct comparison to theory difficult, particularly in the case of high- T_c superconductors. It would therefore be helpful to study a compound with similar many-body physics and a similar MIT but with a simpler spectral function. Here, we report on the ARPES-derived spectral functions of the layered oxide $\text{Bi}_{2-x}\text{Pb}_x\text{M}_2\text{Co}_2\text{O}_8$, with $M=\text{Sr}, \text{Ba}, \text{Ca}$. The spectral functions of these compounds appear to allow for a qualitative comparison to popular many-body models and indicate important trends as a function of temperature and doping.

Doping can cause a MIT in a d -band Mott insulator in two ways.¹ The first is charge doping to change the electron filling level. The second is isoelectronic chemical doping to alter the U/W ratio, where U is the on-site Coulomb repulsion and W is the bandwidth. Both types of doping can be done in this family of cobalt oxides. Theoretically, models for this transition typically fall into one of two categories. One category starts from a description of the insulating state based on the Hubbard Hamiltonian. In the Hubbard picture,² reducing U/W causes the gap between the upper and lower Hubbard bands to close and a transition to a metal occurs when the bands overlap. The other category, the Brinkman-Rice picture, starts from the metallic phase. Here, the quasi-particle (QP) band at E_F narrows and loses spectral weight as the transition is approached.³ Developed more recently, the dynamical mean field theory (DMFT) bridges these two approaches.⁴ As we show here, spectral functions from the DMFT method are remarkably similar to those we have measured in the cobalt oxides.

The structure and composition of the layered compounds of the type Bi-Pb-M-Co-O ($M=\text{Sr}, \text{Ba}, \text{Ca}$) had been the sub-

ject of some debate. Earlier work had identified the compounds as having a structure similar to the superconductor $\text{Bi}_2\text{Sr}_2\text{CaCu}_2\text{O}_8$ (Bi2212). Our previous work on one member of this family labeled the compound as $(\text{Bi}_{0.5}\text{Pb}_{0.5})_2\text{Ba}_3\text{Co}_2\text{O}_y$.⁵ However, the structure and composition of these compounds have since been resolved. The composition is close to $\text{Bi}_{2-x}\text{Pb}_x\text{M}_2\text{Co}_2\text{O}_8$. The structure consists of rocksalt layers of Bi(Pb)MO_2 interspersed with misfit hexagonal layers of CoO_2 .⁶⁻⁸ In general, samples with $M=\text{Ba}$ are more conducting than those with $M=\text{Sr}$; such doping is charge neutral and should be considered as primarily changing U/W . For a given M atomic species, increasing the amount of Pb substituted for Bi increases the conductivity. It is believed that adding Pb increases the number of carriers, thus is primarily charge doping.⁶

The Co ions appear to be in the low spin state as measured by susceptibility⁷ and core level photoemission.⁹ The Co oxidation state in a Pb-free $M=\text{Sr}$ sample has been calculated to be 3.33.¹⁰ Thus, it is unlikely that any of the compounds studied here are at half-filling, though many are strongly insulating. The more metallic samples are typically in-plane metallic and out-of-plane insulating at room temperature, metallic in all directions below some crossover temperature near 150 K, and have an upturn in resistivity in all directions at the lowest temperatures.^{5,7} Previous ARPES work by other groups is broadly consistent with the data we report, but does not detect the sharp, slowly dispersing peak near E_F . Our previous ARPES work has shown the emergence of a sharp peak at E_F tied to a change in the c -axis resistivity from insulating ($dp/dT < 0$) to metalliclike ($dp/dT > 0$).⁵ For $M=\text{Sr}$ and no Pb doping, resistivity in the insulating low temperature phase shows nearly activated behavior. In the same family, for Pb content over 0.4, the low temperature resistivity indicates variable range hopping.¹⁰

Single crystals of $\text{Bi}_{2-x}\text{Pb}_x\text{M}_2\text{Co}_2\text{O}_8$ with $M=\text{Sr}$ or Ba were synthesized using the flux technique as described elsewhere.¹¹ For convenience, we list the samples as M/x in order to describe both the cation and the Pb doping level. Thus, $\text{Sr}/0.52$ indicates $\text{Bi}_{1.48}\text{Pb}_{0.52}\text{Sr}_2\text{Co}_2\text{O}_8$. The sample la-

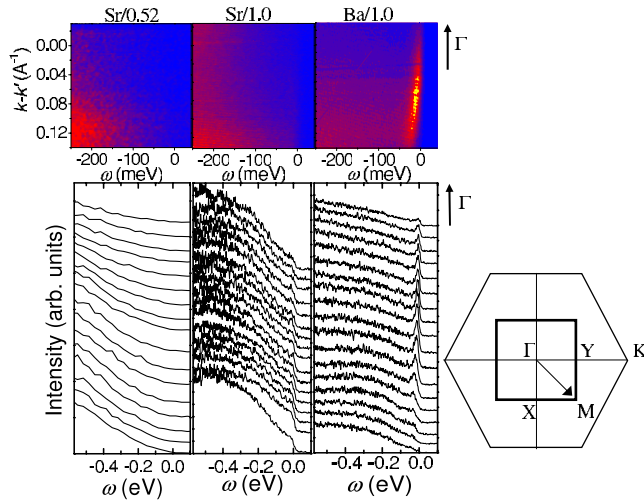


FIG. 1. (Color online) ARPES intensity for sample Sr/0.52 ($T = 50$ K, left column), Sr/1.0 ($T = 40$ K, middle), and Ba/1.0 ($T = 30$ K, right). The top panels are the 2D intensity as a function of energy ω and momentum k measured from $k' = k_F$, where $k = k_F$, the Fermi wave vector for sample Sr/1.0. The bottom panels are the corresponding EDC's over the same k range. The panel in the bottom right is the first Brillouin zone for this structure. The thick line indicates the zone for the (Bi,Pb)MO₂ rocksalt layer, while the larger, lighter line indicates the first Brillouin zone for the hexagonal CoO₂ layers. The data shown here were taken along the Γ to M direction for the rocksalt layers as indicated.

beled Ba/1.0 is the same sample we studied previously in Ref. 5 and labeled as $(\text{Bi}_{0.5}\text{Pb}_{0.5})_2\text{Ba}_3\text{Co}_2\text{O}_y$. Resistivity measurements for both in-plane and out-of-plane transport were made using a conventional four-point probe technique on samples from the same crystal batch as those used in the ARPES measurements. All ARPES measurements were performed at Beamline U13UB of the National Synchrotron Light Source, with photon energies of 15 and 21.2 eV. The end station includes a Scienta SES-200 hemispherical analyzer equipped for simultaneous collection of photoelectrons as a function of energy and angle. The crystals were cleaved *in situ* under vacuum with a base pressure of 1×10^{-10} Torr. The total energy resolution was ~ 15 meV and momentum resolution better than 0.02 \AA^{-1} .

Figure 1 shows the photoemission intensity near E_F along the rocksalt cube-edge direction for a set of cobalt oxide samples. There is some variation in the dispersion in other directions, but the line shapes are essentially the same. The data are plotted both as two-dimensional intensity maps as collected as well as energy dispersion curves (EDC's) at several k values. The leftmost panel is sample Sr/0.52, which is the most insulating of those examined here. Not surprisingly, there is no weight at E_F and a very broad feature with no discernible dispersion. The middle panel is sample Sr/1.0. This sample is charge doped with respect to Sr/0.52 shown in the leftmost panel and is barely metallic, with details of the conductivity below. This sample has developed a barely discernible peak at E_F with slight dispersion. The rightmost panel is Ba/1.0. This is the most metallic of those studied here. The change from the Sr/1.0 in the middle panel in-

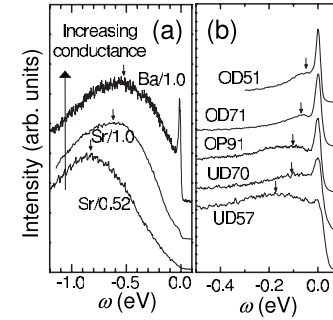


FIG. 2. (a) Broad EDC spectra of cobaltates, samples and temperatures as in Fig. 1. (b) EDC spectra of Bi2212 cuprates near the $(\pi, 0)$ region in the superconducting state. UD69 is underdoped cuprate with $T_c = 69$ K, OP91 is optimally doped with $T_c = 91$ K, and OD51 is overdoped with $T_c = 51$ K. For comparison, each spectrum has been normalized to the energy and intensity of the sharp peak. In both panels, the small arrows locate the visual estimate of the maximum intensity of the broad incoherent peaks.

volves substitution of Ba for Sr, and thus decreasing U/W . In the near E_F region, we see a more intense peak with slightly larger dispersion. This peak appears to cross the Fermi energy such that $k_F \cong 0.5 \text{ \AA}^{-1}$. The existence of a sharp, slowly dispersing peak in the metallic samples that weakens as the insulator is approached is reminiscent of the Brinkman-Rice state approaching the insulator with increasing U/W .³

Figure 2(a) displays the EDC's of the same samples from Fig. 1 over a broader energy range and in a manner suitable for sample to sample comparison. The position and extent of the broad, incoherent part of the excitation are more easily seen here. The spectra are arranged in order of increasing room temperature conductance [marked by the long arrow in Fig. 2(a)]: the bottom spectrum is for the least conducting Sr/0.52 sample, the middle spectrum is for the Sr/2.0 sample showing intermediate conductance, and the top spectrum is for the most conducting Ba/1.0 sample. From the bottom spectrum to the middle, the predominant change is an increase in the number of carriers. From the middle spectrum to the top, the predominant change is a decrease in U/W . The broad peak moves toward E_F with increasing conductivity regardless of the nature of the doping involved. The largest change is associated with adding charge carriers, presumably connected with a change in the chemical potential as in semiconductors. As mentioned above, upon changing the number of carriers in samples that are already basically conducting, there is a small change in the position of the incoherent states but a large increase in the spectral weight of the sharp, quasiparticle related peak at E_F .

There is a close connection between the spectral line shape at E_F and the resistivity measurements. For Sr/0.52, the spectra consist of the broad, incoherent peak and a lack of any intensity at E_F . This corresponds with the insulating behavior in all directions of the temperature-dependent resistivity.^{7,11} In Sr/1.0, the spectra are still dominated by the broad incoherent peak, but a finite intensity develops at E_F with a weak coherent peak. As shown in Fig. 3(b), this sharp peak diminishes with increasing temperature, and is no longer detected above 130 K. Figure 3(a) shows that in-plane

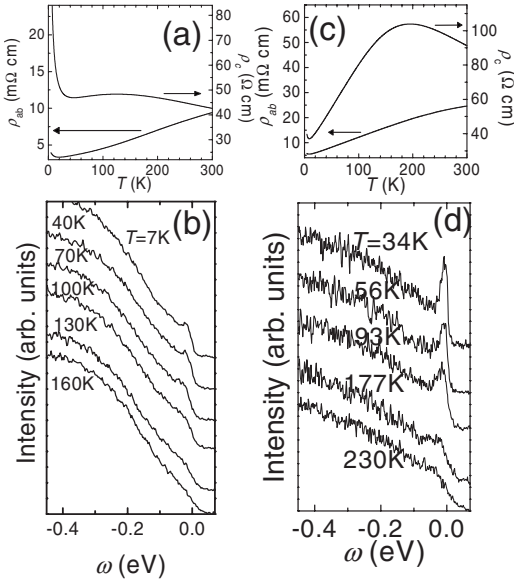


FIG. 3. Temperature-dependent behavior of ρ_{ab} and ρ_c (top panels), and the ARPES spectra (bottom panels) for samples [(a) and (b)] Sr/1.0 and [(c) and (d)] Ba/1.0.

ρ_{ab} is metallic over the temperature range studied, while ρ_c shows predominantly insulating behavior with a crossover to weakly metallic behavior below 120 K. The downturn in ρ_c corresponds to the crossover temperature where the sharp peak in the ARPES spectra appears. Figures 3(c) and 3(d) show similar behavior, but with more pronounced peaks and a more pronounced turnover to metallic temperature dependence for ρ_c , at slightly higher temperature. These characteristics are consistent with those described in our earlier paper⁵ which included measurements on a Ba/1.0-type sample. In both metallic samples, the presence of the coherent, sharp peak in the spectra corresponds to the metallic behavior of ρ_c , whereas the metallic behavior of ρ_{ab} corresponds to the presence of a nonzero intensity in the spectra at the E_F .

Our previous paper established a connection between the temperature-dependent behavior of ρ_{ab} and ρ_c with the effective dimensionality of the system.⁵ A three-dimensional (3D) system is defined as having ρ_{ab} with similar temperature dependence as ρ_c , i.e., ρ_{ab}/ρ_c is nearly constant. Hence, sample Ba/1.0 is essentially 3D below 150 K since both ρ_{ab} and ρ_c have similar behavior ($d\rho/dT > 0$). On the other hand, above 200 K, the sample shows two-dimensional (2D) properties since ρ_{ab} and ρ_c have opposite behavior. The nature of the charge carriers in this 2D phase is unknown but appears to be non-Fermi-liquid. In all cases, the lowest temperature phase appears to be 3D in nature, whether metallic or insulating. This is reminiscent of the high- T_c superconductors such as $\text{La}_{2-x}\text{Sr}_x\text{CuO}_4$, where measurement of the resistivity at low temperatures in the normal state induced by large magnetic fields has shown ρ_{ab} and ρ_c to turn insulating for less than optimal doping.¹²

In some sense, the MIT described here has two parts. As a function of doping, at room temperature, the resistivity data indicate an in-plane transition. The resistivity has taken on a metallic character. However, even in the most metallic samples, the out-of-plane resistivity does not become metal-

lic until below the dimensional crossover temperature. We are not aware of a quantitative model that accounts for this sort of two-part MIT. However, the ARPES spectra themselves have a strong resemblance to the spectral functions calculated within the framework of the infinite-dimensional DMFT for a reasonable range of parameters.^{13,14} A comparison of Fig. 7 vs Fig. 12 of Pruschke *et al.*¹⁴ shows the MIT as a function of carrier concentration. Pruschke *et al.* give the spectral functions in Fig. 7 (for half-filling and $U=3$) and Fig. 12 (for hole doping of 0.03 and $U=3$). Experimentally, a similar variation is observed going from Sr/0.52 to Sr/1.0. The differences are that our lower level of doping is not half-filling and U in our samples is large enough so that there is a gap in the lesser-doped material. Aspects of our data that seem to match the calculation include the ubiquitous presence of a broad high energy excitation, a tendency for the broad peak to sharpen and move to lower energy with increasing conductivity, and the formation of a slowly dispersing sharp peak in the metallic state. The agreement for Sr/1.0 extends to the region of low filling and high temperatures in which the calculated spectra have states at E_F but no QP peak. Further, changes between Sr/1.0 and Ba/1.0 are largely a function of changing U/W . While it is difficult to find a study that explicitly examines the spectral function as a function of U/W away from half-filling, the trends can be seen in studies at half-filling. Both Figs. 16 and 18 of Ref. 4 show the evolution of the spectral function as a function of U/W . The trends match our data in showing a substantial increase in the spectral weight of the sharp peak near E_F with decreasing U/W as well as significant lowering of the energy position of the broad, incoherent peak. The most striking agreement between our data and the DMFT calculated spectral functions is for the temperature dependence of our most conducting sample, Ba/1.0, as shown in Fig. 3(d) here and Fig. 2 of Ref. 5, compared to Fig. 12 of Ref. 14.

The connection between the conductivity data and the DMFT calculations is less clear. The calculations indicate that the disappearance of the sharp peak in the density of states with increasing temperature corresponds to a transition to insulating isotropic resistivity at half-filling (Figs. 12 and 14 of Ref. 14). This is what we observe for ρ_c for the metallic phases.⁵ The measured behavior of ρ_{ab} , i.e., that it remains metallic with no indication of the crossover, is not present in the DMFT calculations.

There are similarities between the spectral function for the cuprate superconductor Bi2212 and these cobaltates. Unlike the cobaltates, the cuprate spectral line shapes are strongly anisotropic within the plane, at least for optimal or lesser doping. The cuprate spectra in the vicinity of the M point are qualitatively similar to the spectra of the cobaltates.¹⁵ In Fig. 2(b), we plot the spectra obtained for Bi2212 at different doping levels: underdoped ($T_c=69$ K), optimally doped ($T_c=91$ K),¹⁶ and overdoped ($T_c=51$ K).¹⁷ The cuprate spectra are taken in the superconducting state near the M point of the Brillouin zone. The spectra are arranged such that the top spectra come from the most conducting compound (OD51), while the bottom spectra are from the least conducting sample (UD69).¹⁸ The two overall patterns that were observed in the cobaltates are repeated here for the cuprates. With increasing conductivity of the sample, the broad hump

sharpens and shifts to lower energies, while the intensity of the sharp peak increases. In both cases, the spectral evolution is consistent with that expected from DMFT calculations and it appears that the appearance of QP states corresponds with the emergence of isotropic electronic behavior.

A possible caveat to the above observation is that some literature has attributed the broad peak near the M point in Bi2212 as being due to a second band of the bilayer CuO planes.¹⁹ While there are few band calculations that explicitly consider charge doping, indications are that the splitting of the bilayer bands should be roughly independent of doping.²⁰ Since ARPES results show that the energy difference between the sharp peak and the broad peak clearly shrinks with doping, and the relative spectral weight of the broad peak continuously decreases, we conclude that this broad peak is not predominantly a second, bonding band. On the other hand, the observed doping and temperature dependence of this broad peak is expected if this feature represents the incoherent part of the excitation. In addition, at least one calculation that considers the effects of bilayer split bands explicitly predicts that this broad feature is predominantly due to the incoherent excitation.²¹ The general picture put forward here concerning the relationship between the sharp quasiparticle peak and the broad incoherent peak it emerges from is similar in spirit to a recent work concerning the evolution of the cuprate compounds from Mott insulator to superconductor.²²

Further comparisons may be made with compounds of the type Na_xCoO_2 . For doping near $x=0.35$, these compounds are the precursors to the water intercalated superconductors with $T_C=5$ K. These compounds consist of edge sharing CoO_6 octahedra forming electronically active triangular sheets separated by Na layers and water in the hydrated versions. They thus have a structure similar to that of the cobaltate compounds discussed here. For heavily doped samples $\text{Na}_{0.7}\text{CoO}_2$, the electronic structure near the Fermi level is very similar to that reported here for the most conducting compounds, $\text{Ba}/1.0$.²³ At low temperatures, $\text{Na}_{0.7}\text{CoO}_2$ exhibits a nearly circular Fermi surface. The corresponding EDC's show a broad (0.6 eV wide) peak located at a binding energy of 0.7 eV, out of which emerges a sharp and weakly dispersive peak at the Fermi level. The temperature dependence of the sharp quasiparticle peak, emerging below $T=120$ K, is similar to that described in this work. In that case, it was reported that this temperature coincides with a change in the in-plane resistivity from T linear at low temperature to a stronger dependence at high temperature. Inter-

estingly, in the lower doped $\text{Na}_{0.3}\text{CoO}_2$, the equivalent quasiparticle peak has a much greater dispersion, perhaps indicating that U/W is much smaller for this latter compound.²⁴ Another group reporting on $\text{Na}_{0.6}\text{CoO}_2$ found dispersion of the quasiparticle peak that was fairly broad, closer to that of $\text{Na}_{0.3}\text{CoO}_2$.²⁵

The dimensional crossover in the resistivity reported here mirrors that seen in some low-dimensional organic compounds but so far those materials have not shown a corresponding emergence of a sharp peak near the Fermi energy. For example, the c -axis transport in the Bechgaard salt $(\text{TMTSF})_2\text{PF}_6$ shows a similar coherent-diffusive crossover as measured here.²⁶ So far, no one has found a correlation of this behavior to ARPES peaks that might represent Fermi-liquid quasiparticles. Generally, sharp peaks near the Fermi energy have not been found in such organic compounds. An example is $(\text{TMTSF})_2\text{ClO}_4$, where no sharp peaks were found near the Fermi energy at $T=150$ K.²⁷ However, a study of $(\text{TMTSF})_2\text{PF}_6$ indicated that the surfaces of this compound are heavily damaged by cleaving and the ARPES process.²⁸ It is difficult to know whether such an ARPES signal of dimensional crossover does not exist for these organic compounds or if it is just difficult to detect.

In summary, we have shown ARPES results for the bismuth cobaltates across the MIT. The correlated insulators have broad, nondispersing, incoherent spectra. The nominally metallic samples are more complex with at least two phases: (i) metallic behavior in the plane accompanied by the appearance of a Fermi edge in an otherwise broad spectral function and (ii) at lower temperatures a 3D electronic state occurs accompanied by the transfer of spectral weight to a sharp, slowly dispersing quasiparticle peak. As conductivity increases from sample to sample, either through increasing the number of holes or decreasing U/W , the broad incoherent part of the spectrum sharpens and shifts toward the Fermi energy and the sharp peak increases in intensity. The spectral function near the ΓM region of the Bi2212 superconducting compounds evolves similarly. Despite the prominence of a phase that is metallic in plane and insulating out of plane, the zero temperature phase for all of the layered compounds appears to be 3D in nature.

We acknowledge valuable discussions with V. Perebeinos, A. Tsvelik, J. Tu, and R. Werner. This work was supported in part by the Department of Energy under Contracts No. DE-AC02-98CH10886, No. DE-FG02-00ER45801, and No. DOE-BES W-31-109-ENG-38. B.O.W. acknowledges the support of the Cottrell Scholar Fellowship.

*Present address: High Energy Physics Division, Argonne National Laboratory, Argonne, IL 60439.

†Present address: ALS, Lawrence Berkeley National Laboratory, Berkeley, CA 94720.

¹A. Fujimori, T. Yoshida, K. Okazaki, T. Tsujioka, K. Kobayashi, T. Mizokawa, M. Onoda, T. Katsufuji, Y. Taguchi, and Y. Tokura, *J. Electron Spectrosc. Relat. Phenom.* **117-118**, 277

(2001).

²J. Hubbard, *Proc. R. Soc. London, Ser. A* **281**, 401 (1964).

³W. F. Brinkman and T. M. Rice, *Phys. Rev. B* **2**, 4302 (1970).

⁴A. Georges, G. Kotliar, W. Krauth, and M. J. Rozenberg, *Rev. Mod. Phys.* **68**, 13 (1996).

⁵T. Valla, P. D. Johnson, Z. Yusof, B. Wells, Q. Li, S. M. Loureiro, R. J. Cava, M. Mikami, Y. Mori, M. Yoshimura, and T. Sasaki,

- Nature (London) **417**, 627 (2002).
- ⁶T. Yamamoto, K. Uchinokura, and I. Tsukada, Phys. Rev. B **65**, 184434 (2002).
- ⁷I. Tsukuda, T. Yamamoto, M. Takagi, T. Tsubone, S. Konno, and K. Uchinokura, J. Phys. Soc. Jpn. **70**, 834 (2001).
- ⁸TEM studies in the group of R. J. Cava have confirmed a CoO hexagonal layer.
- ⁹T. Mizokawa, L. H. Tjeng, P. G. Steeneken, N. B. Brookes, I. Tsukada, T. Yamamoto, and K. Uchinokura, Phys. Rev. B **64**, 115104 (2001).
- ¹⁰T. Yamamoto, I. Tsukada, K. Uchinokura, M. Takagi, T. Tsubone, M. Ichihara, and K. Kobayashi, Jpn. J. Appl. Phys., Part 2 **39**, L747 (2000).
- ¹¹S. M. Loureiro, D. P. Young, R. J. Cava, R. Jin, Y. Liu, P. Bordet, Y. Qin, H. Zandbergen, M. Godinho, M. Núñez-Regueiro, and B. Batlogg, Phys. Rev. B **63**, 094109 (2001).
- ¹²G. S. Boebinger, Y. Ando, A. Passner, T. Kimura, M. Okuya, J. Shimoyama, K. Kishio, K. Tamasaku, N. Ichikawa, and S. Uchida, Phys. Rev. Lett. **77**, 5417 (1996).
- ¹³M. J. Rozenberg, R. Chitra, and G. Kotliar, Phys. Rev. Lett. **83**, 3498 (1999).
- ¹⁴Th. Pruschke, D. L. Cox, and M. Jarrell, Phys. Rev. B **47**, 3553 (1993).
- ¹⁵We note that the cuprate electronic structure is highly anisotropic. The spectra of the cuprates only along the Cu–O bond direction (ΓM) show similar line shapes with the cobaltates. This is the region that determines the c -axis transport of the cuprates.
- ¹⁶A. V. Fedorov, T. Valla, P. D. Johnson, Q. Li, G. D. Gu, and N. Koshizuka, Phys. Rev. Lett. **82**, 2179 (1999).
- ¹⁷Z. M. Yusof, B. O. Wells, T. Valla, A. V. Fedorov, P. D. Johnson, Q. Li, C. Kendziora, Sha Jian, and D. G. Hinks, Phys. Rev. Lett. **88**, 167006 (2002).
- ¹⁸C. Kendziora, R. J. Kelley, E. Skelton, and M. Onellion, Physica C **257**, 74 (1996).
- ¹⁹D. L. Feng, C. Kim, H. Eisaki, D. H. Lu, A. Damascelli, K. M. Shen, F. Ronning, N. P. Armitage, N. Kaneko, M. Greven, J.-I. Shimoyama, K. Kishio, R. Yoshizaki, G. D. Gu, and Z.-X. Shen, Phys. Rev. B **65**, 220501(R) (2002); Y.-D. Chuang, A. D. Gromko, A. Fedorov, Y. Aiura, K. Oka, Y. Ando, H. Eisaki, S. I. Uchida, and D. S. Dessau, Phys. Rev. Lett. **87**, 117002 (2001); P. V. Bogdanov, A. Lanzara, X. J. Zhou, S. A. Kellar, D. L. Feng, E. D. Lu, H. Eisaki, J.-I. Shimoyama, K. Kishio, Z. Hussain, and Z. X. Shen, Phys. Rev. B **64**, 180505(R) (2001).
- ²⁰A. I. Liechtenstein, O. Gunnarsson, O. K. Andersen, and R. M. Martin, Phys. Rev. B **54**, 12505 (1996). See Fig. 5.
- ²¹M. Eschrig and M. R. Norman, Phys. Rev. Lett. **89**, 277005 (2002).
- ²²K. M. Shen, F. Ronning, D. H. Lu, W. S. Lee, N. J. C. Ingle, W. Meevasana, F. Baumberger, A. Damascelli, N. P. Armitage, L. L. Miller, Y. Kohsaka, M. Azuma, M. Takano, H. Takagi, and Z.-X. Shen, Phys. Rev. Lett. **93**, 267002 (2004).
- ²³M. Z. Hasan, Y.-D. Chuang, D. Qian, Y. W. Li, Y. Kong, A. Kuprin, A. V. Fedorov, R. Kimmerling, E. Rotenberg, K. Rossnagel, Z. Hussain, H. Koh, N. S. Rogado, M. L. Foo, and R. J. Cava, Phys. Rev. Lett. **92**, 246402 (2004).
- ²⁴M. Z. Hasan, D. Qian, Y. Li, A. V. Fedorov, Y.-D. Chuang, A. P. Kuprin, M. L. Foo, and R. J. Cava, Ann. Phys. (N.Y.) **321**, 1568 (2006).
- ²⁵H.-B. Yang, S.-C. Wang, A. K. P. Sekharan, H. Matsui, S. Souma, T. Sato, T. Takahashi, T. Takeuchi, J. C. Campuzano, R. Jin, B. C. Sales, D. Mandrus, Z. Wang, and H. Ding, Phys. Rev. Lett. **92**, 246403 (2004).
- ²⁶G. Mihály, I. Kézsmárki, F. Zámbarczy, and L. Forró, Phys. Rev. Lett. **84**, 2670 (2000).
- ²⁷F. Zwick, S. Brown, G. Margaritondo, C. Merlic, M. Onellion, J. Voit, and M. Grioni, Phys. Rev. Lett. **79**, 3982 (1997).
- ²⁸M. Sing, U. Schwingenschlögl, R. Claessen, M. Dressel, and C. S. Jacobsen, Phys. Rev. B **67**, 125402 (2003).